Journal of Hydrology: Regional Studies 34 (2021) 100786

Contents lists available at ScienceDirect

Journal of Hydrology: Regional Studies

journal homepage: www.elsevier.com/locate/ejrh

Characterization of the isotopic composition and bulk ion deposition of precipitation from Central to West Hawai'i Island between 2017 and 2019

Diamond K. Tachera [a,b,*], Nicole C. Lautze [b], Giuseppe Torri [c], Donald M. Thomas [b]

[a] Department of Earth Sciences, School of Ocean and Earth Science and Technology, University of Hawai'i at Mānoa, 1680 East-West Road, POST 602, Honolulu, HI, 96816, USA
[b] Hawai'i Institute of Geophysics and Planetology, School of Ocean and Earth Science and Technology, University of Hawai'i at Mānoa, 1680 East-West Road, POST 602, Honolulu, HI, 96816, USA
[c] Department of Atmospheric Sciences, School of Ocean and Earth Science and Technology, University of Hawai'i at Mānoa, 2525 Correa Road, HIG 338, Honolulu, HI, 96816, USA

ARTICLE INFO

Keywords:
Stable isotopes
Bulk deposition
Precipitation
Groundwater
Hawaii Island
Local meteoric water line

ABSTRACT

Study region: The current study evaluates the isotopic and chemical compositions of rainfall from central to leeward Hawai'i Island, an area characterized by the interactions of Pacific trade wind flow with two 4,000-meter high mountains as well as one of the largest natural emitters of sulfur dioxide on the planet.
Study focus: Our study collected cumulative rainfall samples at regular intervals over a 28-month period from 20 stations spanning a range of elevations across this region and determined average isotopic and dissolved ion compositions in those samples. The study period included an extreme weather event (Hurricane Lane), a major volcanic eruption at Kīlauea in 2018, and the nearly complete cessation of long-term volcanic emissions following that eruptive event.
New hydrological insights: to the Region Consistent with previous literature, results show long-term variability through our establishment of an enhanced local meteoric water line (LMWL) for West Hawai'i. We hypothesize the two LMWL represent ends of a spectrum, due to the variability in atmospheric and climate processes in this region. Additionally, results of stable isotope compositions and bulk ion deposition highlight how extreme events, such as volcanic eruptions and hurricanes, can affect the chemistry of precipitation. Sulfate concentrations in bulk precipitation decreased by a mean of 70 % ($p = 0.032$) after the 2018 Kīlauea eruption ceased. The results from this study can be used to better quantify and characterize precipitation, which is the ultimate source of Hawai'i's groundwater.

1. Introduction

Groundwater is the main source of potable water in the State of Hawai'i. To better understand the spatial distribution of groundwater recharge on Hawai'i Island, we look to the source - precipitation. Understanding the source of Hawai'i's groundwater is critical to future water security. Questions including the degree of connectivity between aquifers, and the sustainability of

* Corresponding author.
E-mail address: diamondt@hawaii.edu (D.K. Tachera).

https://doi.org/10.1016/j.ejrh.2021.100786
Received 30 September 2020; Received in revised form 26 January 2021; Accepted 29 January 2021
Available online 16 February 2021

groundwater withdrawal, continue to puzzle hydrogeologists and draw concerns from growing communities and water managers across the State, including West Hawai'i. Complex subsurface geologic structures in West Hawai'i Island are inferred, which require further investigation (Oki, 1999; Tillman et al., 2014; Kelly and Glenn, 2015; Attias et al., 2020). Building upon other studies (e.g., Fackrell et al., 2020), we investigate the variable chemistry of precipitation from Central to West Hawai'i Island given its link to source, storage, and flow of groundwater.

This research is part of the National Science Foundation, EPSCoR Track 1 'Ike Wai project. A key science goal of 'Ike Wai is to investigate groundwater recharge, storage, and flow within an ocean island volcanic enivornment. 'Ike Wai collected, and is currently analyzing, new geophysical, microbiological, and geochemical data in the West Hawai'i study region. The objective of this paper specifically, is to investigate isotopic and bulk ion deposition variability in precipitation across an extended region of Central and West Hawai'i Island. Here we present results from precipitation samples collected at 20 sites on an approximately quarterly basis between August 2017 and November 2019 (Fig. 1). During the 28-month sampling period, Kīlauea Volcano experienced a large-volume East Rift Zone eruption from early May to September 2018 that, at its conclusion, terminated a ~35 year period of nearly continuous eruptive activity at Kīlauea. Hurricane Lane impacted the State of Hawai'i and specifically Hawai'i Island in late August 2018. These events allowed us the rare opportunity to investigate the impact of volcanic gases (also known as vog) and a hurricane, respectively, on the precipitation chemistry.

The stable isotopes of water, ^{18}O and ^{2}H (also referred to as deuterium or D), have been used around the world to identify the source and flow trajectories of water. The global meteoric water line (GMWL) is a linear trendline that describes the majority of precipitation that falls on Earth by relating $\delta^{18}O$ and δD as $\delta D = 8\,\delta^{18}O + 10$ (Craig, 1961). Two main factors that control the isotopic composition of precipitation are the temperature of condensation and the amount of rainout from the air mass (Dansgaard, 1964). Seasonal variations in $\delta^{18}O$ and δD precipitation values at tropical latitudes can be attributed to the source of moisture and to the amount effect, as well as elevation and types of convection (Torri et al., 2017). These variations remain fairly constant at tropical latitudes due to their consistent annual climatic patterns (Dansgaard, 1964).

A first publication on the stable isotope variations in Hawai'i rainfall was by Friedman and Woodcock (1957), and focused on East Hawai'i Island. More recent work in Hawai'i has been conducted in the Kīlauea Region of Hawai'i Island, on Haleakalā on Maui, on the island of O'ahu, and in West Hawai'i Island (Scholl et al., 1996, 2002; Tillman et al., 2014; Fackrell et al., 2020; Dores et al., 2020). This research expands on the work of Fackrell et al. (2020) in West Hawai'i. Between October 2012 and December 2014, Fackrell et al. (2020) collected and analyzed isotopic compositions of precipitation recovered at six-month collection intervals from eight sites and produced a local meteoric water line (LMWL) for the West Hawai'i region. Using the LMWL in conjunction with groundwater data, their study determined recharge elevations to develop new conceptual models for groundwater flow paths. One of their conclusions is the suggestion that precipitation from high elevations on Mauna Kea and Mauna Loa volcanoes recharge the Hualālai aquifers. However, no data were collected from the high-elevation regions, demonstrating the need for an expanded investigation in order to more fully comprehend the complex hydrogeology of West Hawai'i.

Precipitation studies focusing on chemical composition, pH, and the effects of Kīlauea gases on acid rain have been conducted on Hawai'i Island for more than six decades (Eriksson, 1957; Miller and Yoshinaga, 1981; Harding and Miller, 1982; Nachbar-Hapai et al., 1989; Siegel et al., 1990; Scholl and Ingebritsen, 1995). Similar coastal and volcanic studies of wet and bulk (wet + dry) deposition of

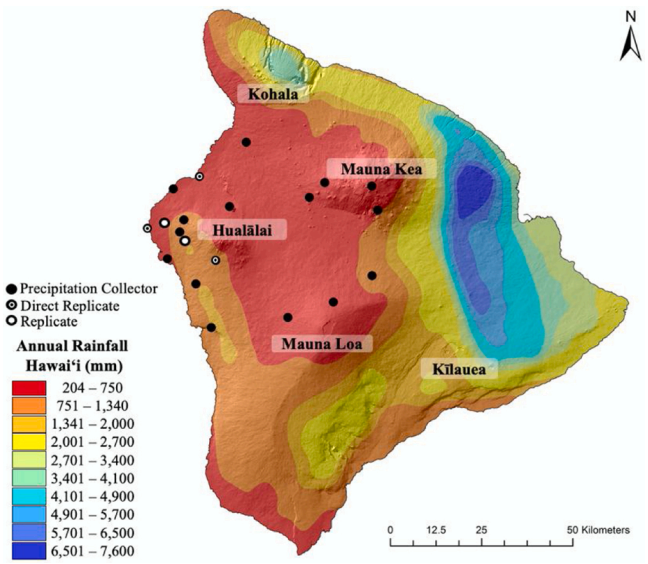

Fig. 1. Twenty precipitation collectors (black points) were deployed throughout the West Hawai'i study area, extending into Central Hawai'i Island on Mauna Kea and Mauna Loa volcanoes. Five replicated sites from the Fackrell et al. (2020) study are shown, three as direct replicates and two replicates to within two kilometers and 100 m elevation. The base map shows average annual rainfall contours for Hawai'i Island (Giambelluca et al., 2013); the five volcanoes of Hawai'i Island are labeled.

major ions in precipitation have been conducted around the world, such as in Mexico (Cerón et al., 2005), Korea (Lee et al., 2000), and Italy (Aiuppa et al., 2006). A study by Zuo et al. (2020) used rainfall and vog emission observations in a numerical model to demonstrate that increased aerosols from Kīlauea Volcano have reduced rainfall for the downwind regions of Hawai'i Island.

Although challenging to collect, we contend that long-term precipitation geochemistry data over a broad area of Hawai'i Island are needed to develop a LMWL that is able to characterize the isotopic composition of rainfall recharge and its evolution to local groundwater. This paper provides the most comprehensive such dataset to date.

2. Material and methods

2.1. Study site

There are three volcanoes located within the West Hawai'i study region: Hualālai, Mauna Kea, and Mauna Loa (Fig. 1). Hualālai volcano is the western-most volcano on Hawai'i Island, standing at an elevation of 2,523 m above mean sea level (amsl). Although the age of Hualālai versus Mauna Kea has been debated over time (Moore and Clague, 1992), the most recent research identifying the superposition of shore breaks supports that Hualālai is older (Taylor, 2019). Mauna Loa is one of the most voluminous volcanoes on the planet, rising to 4,169 m amsl. Mauna Kea is slightly taller, standing at 4,207 m amsl. Hualālai and Mauna Loa are considered volcanically active, and all three volcanoes have surface lava flows that extend to the coast within the study area.

The study area experiences a diverse range of climates. Mean annual air temperatures range from 22−24 °C in coastal regions to 4−6 °C in the high summit regions of Mauna Loa and Mauna Kea (Giambelluca et al., 2014). Due to Hualālai's placement in the rain shadow of Mauna Kea and Mauna Loa, trade wind-derived orographic precipitation does not reach this region. Instead, land-breeze sea-breeze patterns are experienced almost daily. Annual rainfall averages for Hawai'i Island range from 204 mm to 2,750 mm (Giambelluca et al., 2013). The Kona coffee region of Kailua-Kona has a unique pattern of rainfall, with a band of higher rainfall at mid-elevations (300 m–500 m amsl) (Fig. 1). Airflow travels from the eastern side of Hawai'i Island (Kīlauea) around the southern tip and back up the western slopes of Mauna Loa, causing a persistent band of clouds and rain almost daily (Giambelluca et al., 2013). Afternoon land breezes typically enhance the cloud belt. West Hawai'i experiences more intense rain events during the summer months, in contrast with much of the rest of the State of Hawai'i, which experiences the most rain in the winter (Leopold, 1949). Precipitation above the trade wind inversion, found at around 2,000 m, decreases steeply with elevation, resulting in a dry environment that receives rain dominantly from extra-tropical and subtropical storms (Giambelluca et al., 2013).

Kīlauea is the eastern-most volcano on Hawai'i Island and has, until recently, been in a state of nearly continous eruption for more than 35 years. Volcanic gases emitted by Kīlauea are dominantly carbon dioxide (CO_2), sulfur dioxide (SO_2), hydrogen sulfide (H_2S), and hydrogen halides (HF, HCl, HBr) and are distributed throughout Hawai'i by varying weather systems (Sutton and Elias, 2014). From 1983–2018, eruptive activity occurred along Kīlauea's East Rift Zone as well as at the summit, where a lava lake at Halema'uma'u crater produced heavy gas plumes between 2008 and 2018 (Neal and Anderson, 2020). Kīlauea erupted on its Lower East Rift Zone (LERZ) between late May to September 2018, draining the lava lake, causing a more than 10-fold increase in gas emissions and, at the conclusion of that event, bringing a cessation in eruptive activity for the first time in decades (Williams et al., 2020).

Table 1
Precipitation collector site information and VWA results. Replicated sites from the Fackrell et al. (2020) study are denoted with an asterisk, sites within 2 km and approximately 100 m elevation denoted with two asterisks.

Site information						08/2017−11/2019 totals		
Site	Latitude	Longitude	Elevation (m)	Funnel Diameter (mm)	*n*	Cumulative Precipitation (mm)	VWA $\delta^{18}O$ (‰)	VWA $\delta^{2}H$ (‰)
*Kīholo	19.85	−155.92	3	101.6	5	189	−3.6	−18.3
*Keāhole	19.72	−156.05	5	101.6	9	437	−3.2	−15.5
Keahuolū	19.65	−156.00	12	152.4	3	221	−2.3	−5.8
Ka'ūpūlehu	19.82	−155.98	17	101.6	6	514	−2.8	−13.3
**Pālamanui	19.73	−156.01	140	152.4	7	287	−3.2	−15.0
Waikoloa	19.93	−155.79	250	101.6	3	416	−2.5	−7.9
Kealakekua	19.47	−155.89	430	152.4	4	1296	−2.4	−5.9
Kahalu'u	19.58	−155.93	520	152.4	1	612	−2.1	−3.6
Kalaoa	19.71	−155.97	540	101.6	9	1495	−3.2	−12.3
**Kaloko	19.69	−155.96	660	101.6	7	2789	−2.8	−8.3
Hu'ehu'e	19.74	−155.96	730	152.4	6	975	−3.8	−16.4
Pu'u Wa'awa'a	19.77	−155.84	780	101.6	9	1298	−4.4	−23.4
*Hōlualoa	19.64	−155.88	1380	152.4	8	2237	−4.3	−19.2
Ka'ohe	19.79	−155.63	1620	101.6	6	1410	−6.5	−41.9
Pu'u Lā'au	19.83	−155.59	2270	101.6	4	464	−8.5	−58.1
Humu'ula	19.60	−155.47	2430	101.6	7	1651	−6.4	−44.0
Pu'u o Uo	19.50	−155.69	2615	152.4	1	747	−6.4	−36.8
Hale Pōhaku	19.76	−155.45	2840	101.6	5	1000	−10.6	−72.1
Mauna Loa	19.53	−155.57	3400	203.2	7	1033	−10.5	−73.5
Mauna Kea	19.82	−155.47	4200	203.2	3	488	−12.8	−91.5

2.2. Sampling methods

Twenty rain collectors were deployed throughout the study site. Three of our sites exactly replicated, and two were located within two kilometers and 100 m elevation of, Fackrell et al. (2020) sites. Such replicated sites are denoted by single and double asterisks, respectively (Table 1). Samples were collected on an approximately quarterly basis to assess seasonal trends in rainfall, including cumulative volume during the sampling intervals, isotopic composition ($\delta^{18}O$ and δD), and ion chemistry. Two models of rain collectors were used in this study (Fig. 2): 1) NovaLynx Rain and Snow Gauges, which have a 20 cm diameter funnel and are secured in a tripod stand that is bolted to cement platforms, and 2) a hand-made design based on that of previous studies (Scholl et al., 1996; Fackrell et al., 2020), which uses a 5-gallon HDPE bucket with a 101.6 or 152.4 mm diameter funnel protruding from the bucket lid. These bucket-style rain collectors were secured to common potting stands, which were secured into the ground with metal stakes. A 1-cm thick layer of mineral oil was poured into both styles of collectors to prevent rainwater from evaporating. The NovaLynx Gauges were deployed at the UH88 Telescope on the summit of Mauna Kea and at the Mauna Loa Observatory research facility. The hand-made design was deployed at the other 18 sites.

At the time of each sample collection, the weather conditions, temperature, and total volume of water was recorded following methods described in Fackrell et al. (2020). The volumes presented in Tachera (2020) are the measured total volume of precipitation in each collector for each sampling interval (co-located rain gages were not used). Of the total volume, a 500 mL sample in a HDPE bottle was taken for further analyses; the rest was poured out at the site. A 0.2 μm MilliporeSigma Sterile Syringe Filter was used to remove any biological material or mineral oil from the 500 mL sample. Each 500 mL sample was then partitioned into two 60 mL HDPE bottles and refrigerated until sample analysis was conducted, which was typically within two to six weeks of sample collection. One 60 mL bottle was used for major ion and the other for $\delta^{18}O$ and δD analyses.

2.3. Analytical methods

Stable isotopes were analyzed by the Biogeochemical Stable Isotope Facility at the University of Hawai'i at Mānoa. Stable isotope analyses for $\delta^{18}O$ and δD were performed using a Picarro L1102-i wavelength scanned cavity ring down spectroscopy (WS-CRDS) following similar methods as Godoy et al. (2012) relative to V-SMOW. Within our dataset, the minimum standard deviation for $\delta^{18}O$ and δD was 0.01 (‰), and the maximum standard deviation was 0.07 (‰) and 0.59 (‰) for $\delta^{18}O$ and δD, respectively. Major ion analyses for cations (Na, K, Mg, Ca) and anions (F, Cl, Br, SO_4) were performed by the Water Resources Research Center laboratory at the University of Hawai'i at Mānoa using a dual Dionex ICS-1100 Ion Chromatograph following the US EPA Method 300.1 for determining inorganic ions in drinking water (Hautman and Munch, 1997). Sample precision at one standard deviation based on duplicate sample pairs indicate variances of ±0.342 μM (F), ±28.36 μM (Cl), ±0.28 μM (Br), ±18.96 μM (SO_4), ±24.78 μM (Na), ±5.47 μM (NH_4), ±1.40 μM (K), ±13.22 μM (Mg), and ±16.45 μM (Ca).

3. Results and discussion

3.1. Short-term trends in stable isotopes

The accumulated precipitation (mm), $\delta^{18}O$ (‰) and δD (‰) results for each sampling period are presented in Fig. 3 to show the variability in the precipitation rate over time at each site (Tachera, 2020). Of the 20 rain collectors, 9 were visited immediately after Hurricane Lane to collect a hurricane-specific sample. The volume-weighted averages (VWA) of $\delta^{18}O$ and δD values of all the samples

Fig. 2. (a) A NovaLynx Rain and Snow Gauge, deployed at the Mauna Loa Observatory. (b) A bucket-style rain collector, deployed at Humu'ula.

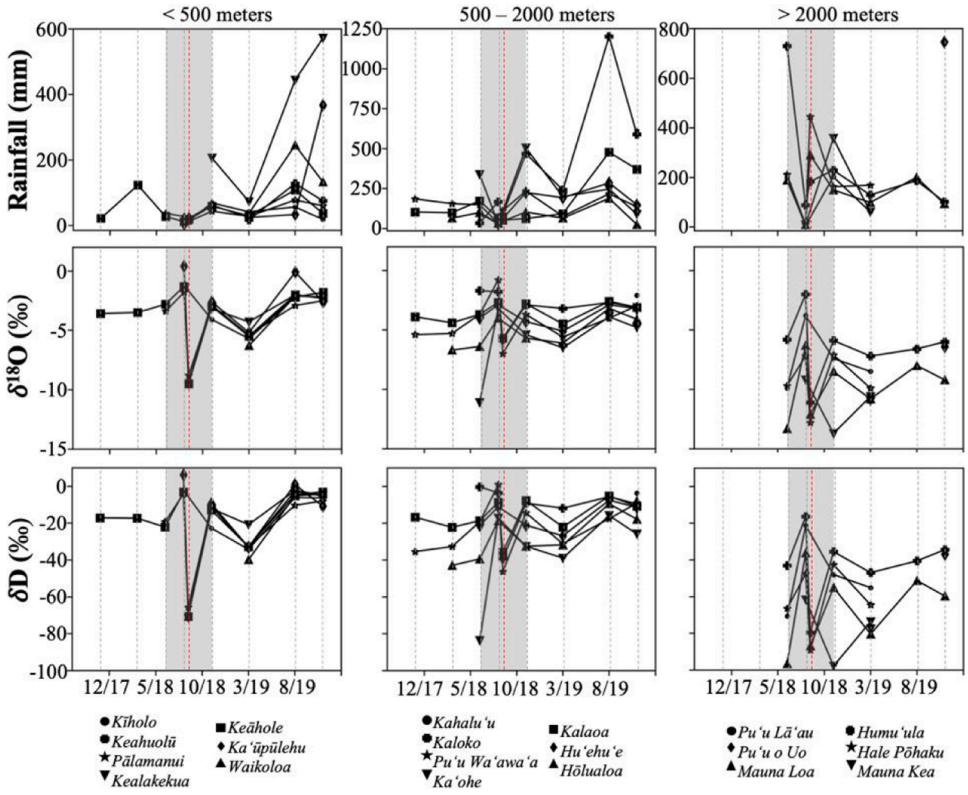

Fig. 3. Precipitation (mm), $\delta^{18}O$ (‰), δD (‰) values for precipitation sites sampled between August 2017 and November 2019. The precipitation sites are broken up into three columns: low elevation sites-less than 500 m (n = 7), mid elevation sites-500 to 2,000 m (n = 7), and high elevation sites-above 2,000 m (n = 6). The first row shows the precipitation accumulated (in mm), the second row shows the $\delta^{18}O$ isotopic composition (‰), and the bottom row shows the δD isotopic composition (‰). The shaded region represents the duration of the 2018 Kīlauea eruption. Dashed vertical lines represent each sample collection, and the red vertical dashed line represents the Hurricane Lane event and sample collection.

collected at each site are shown in Fig. 4 and Table 1. In Fig. 3, the samples are separated as follows: seven "low"-elevation sites below 500 m relative to mean sea level (msl), seven "mid"-elevation sites between 500 and 2,000 m msl, and six "high"-elevation sites above 2,000 m msl. Low-elevation sites are distinguished from those above 500 m because they exhibit similar trends in rainfall (mm) and isotopic composition (Fig. 5). High-elevation sites are separated out because they are above the trade wind inversion that typically

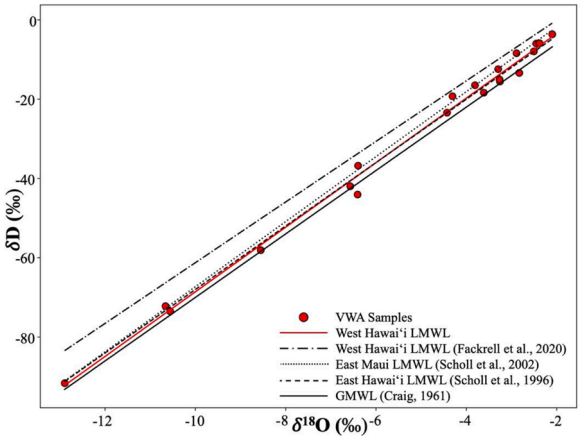

Fig. 4. Volume-weighted averages for the twenty sites, shown as red points. Various local meteoric water lines (LMWL) are displayed: the West Hawai'i LMWL conducted by this study as a solid red line, the West Hawai'i LMWL defined by Fackrell et al. (2020) as a black dot-dash line, the East Maui LMWL defined by Scholl et al. (2002) as a black dotted line, the East Hawai'i LMWL defined by Scholl et al. (1996) as a black dashed line, and the global meteoric water line (GMWL) defined by Craig (1961) as a solid black line.

occurs at around 2,000 m and therefore experiences different patterns of rainfall (Giambelluca et al., 2013). The shaded region in Fig. 5 represents the Kīlauea LERZ eruption from May to September 2018.

Observed quarterly cumulative rainfall at low-elevation sites was less than 250 mm until after the cessation of the 2018 Kīlauea eruption. The rainfall during the eruption period of May to September 2018 was particularly low, as summer is typically the rainy season in West Hawai'i. At these low elevations, isotopic variability throughout the study period is observed with the most depleted isotopic compositions collected during Hurricane Lane. The remaining depleted samples were collected during the dry, winter season possibly indicating that, rather than local storms produced by daily heating, larger storm systems contribute to the rainfall in this region during these months, as was also noticed by Dores et al. (2020).

At mid-elevations, quarterly cumulative rainfall generally peaked at ~500 mm, with one outlier (Kaloko) collecting over 1,000 mm in a sample period. Similar to the low-elevation sites, rainfall remained relatively low throughout the summer of 2018 until the cessation of the Kīlauea eruption. Isotopic variability is observed, with Hurricane Lane not making much of an impact at mid-elevations. Isotopic variability is observed at these elevations, but the impact of Hurricane Lane on isotopic values is more muted here than seen at the lower elevation sites. Similarly, relative seasonal variations in isotopic compositions at the mid-elevations are less than seen at the lower elevations.

At high-elevation sites, quarterly cumulative rainfall appears to be higher during the 2018 Kīlauea eruption, however sampling at Pu'u Lā'au, Hale Pōhaku, and Mauna Kea ended early in March 2019. Also, due to the central location of many of the high-elevation sites on Hawai'i Island, it is likely that these sites are influenced by weather systems that pass over the island, particularly larger more organized systems like cold fronts or Kona lows. High-elevation sites observed the most isotopically depleted compositions overall and the strongest isotopic variability. Similar to the low- and mid-elevation sites, the winter season is observed to have the most depleted samples besides those collected during Hurricane Lane, possibly due to the influence of larger storm systems that originate at higher latitudes that travel toward the islands (e.g., Dores et al., 2020).

The West Hawai'i local meteoric water line was calculated by determining the linear regression through the VWA of $\delta^{18}O$ and δD for all sites, and is described as $\delta D = 8.14\ \delta^{18}O + 12.83$ ($r^2 = 0.99$). The LMWL from this study is nearly identical to the East Hawai'i LMWL, $\delta D = 8.0\ \delta^{18}O + 12$, defined by Scholl et al. (1996) and differs from the LMWL defined for the West Hawai'i region by Fackrell et al. (2020), $\delta D = 7.65\ \delta^{18}O + 15.25$ (Fig. 4). The variability between the LMWL is discussed further in Section 3.2.

The $\delta^{18}O$ (‰) isotope-elevation relationship is shown in Fig. 5. The linear regression is defined as $\delta^{18}O = -0.0017\ h - 2.54$ for low- and mid-elevation sites (lapse rate = -0.17‰/100 m), and $\delta^{18}O = -0.0030\ h - 0.33$ for high-elevation sites (lapse rate = -0.30‰/100 m), where h is the elevation of each site in meters relative to msl. The isotope-elevation relationships observed are similar to those found by Scholl et al. (1996) for trade wind (below 2,000 m) and high-elevation (above 2,000 m) areas. Comparing these regressions and lapse rates to previous studies worldwide, Poage and Chamberlain (2001) compiled 68 studies from around the world and determined a global lapse rate of -0.28‰/100 m; Paternoster et al. (2008) found a similar lapse rate of -0.17‰/100 m for Mt. Vulture, Italy; Kong and Pang (2016) found a positive lapse rate of 0.12‰/100 m for the Tianshan Mountains. The $\delta^{18}O$ lapse rates observed, which are on the low end of the global $\delta^{18}O$ lapse rates, are likely a function of temperature lapse rates and the sources of moisture.

There does not appear to be a strong relationship between elevation and isotopic composition below an elevation of 1,000 m. All of the sites deployed in the lowest annual rainfall zone (Fig. 1) have VWA values that are isotopically depleted relative to the calculated regression lines (Fig. 5). The exceptions are three sites (Keahuolū, Waikoloa, and Pu'u o Uo, Fig. 5 as squares), which are enriched relative to the regression lines despite being located in the lowest annual rainfall zone. It is important to note, however, that these sites collected precipitation for under one year. Previous studies in Hawai'i determined that elevation effects were difficult to observe below

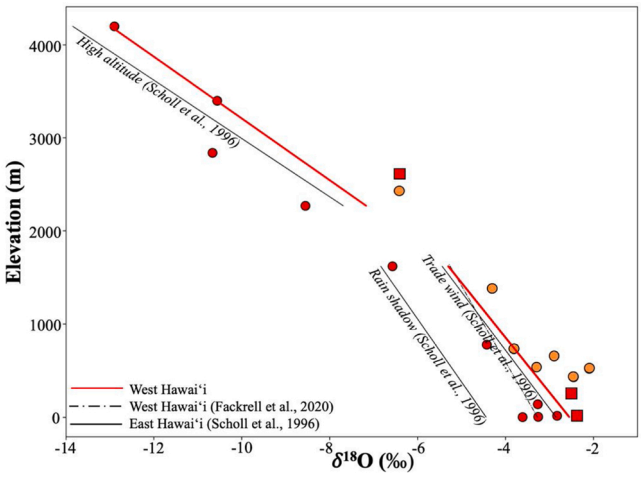

Fig. 5. The VWA $\delta^{18}O$-elevation relationship. Regressions are drawn through the samples below and above the approximately 2,000 m inversion zone for the West Hawai'i dataset. Sites are colored red and orange based on the rainfall zones, 204-750 mm and 751-1,340 mm respectively. Three sites that are enriched relative to the regressions but are within the lowest annual rainfall zone (Fig. 1) are shown as squares. Isotope-elevation relationships observed by Scholl et al. (1996) for Kīlauea region and Fackrell et al. (2020) for the West Hawai'i region are shown for reference.

the inversion layer (Dores et al., 2020). The lowest annual rainfall zone likely only receives rainfall during extratropical and subtropical storm events, which would therefore have already depleted $\delta^{18}O$ isotopic compositions resulting in depleted $\delta^{18}O$ samples compared to the regression lines (Gedzelman and Lawrence, 1990; Good et al., 2014; Dütch et al., 2016).

Precipitation sites that are enriched relative to the linear regression, with the exception of the three mentioned just above, fall within the orange (751−2,000 mm) annual rainfall zone (Fig. 1). Given that rainfall in the orange zone has been interfacing with the land as it travels from the windward to leeward side of the island, it is possible that there may be isotopic enrichment of the water at the base of the cloud (Scholl et al., 2002, 2007). Another explanation for the observed enrichment is that more of the rainfall here occurs in frequent, lower intensity rain events that are related to the diurnal wind cycles and thus is not as depleted - due to the amount effect - as precipitation from infrequent storms that contribute more to the lower elevation red zone. These hypotheses could explain the enrichment of samples above the regression line, however more data are necessary to provide a conclusive answer.

3.2. Comparison of stable isotopes across studies

There is a distinct difference between the LMWL produced by the data of Fackrell et al. (2020) versus this study (Fig. 6), which potentially addresses the discrepancy of ^{18}O enrichment in groundwater samples observed in previous studies (Tillman et al., 2014; Kelly and Glenn, 2015). Fig. 5 of Fackrell et al. (2020) shows that the salinity-corrected groundwater-sample-group averages plot with an offset to the right of the West Hawai'i LMWL, described as $\delta D = 7.65\ \delta^{18}O + 15.25$, indicating an ^{18}O enrichment in groundwater relative to precipitation. They propose four hypotheses for this difference: 1) variability in precipitation δD and $\delta^{18}O$ values during the study period compared to a long-term average, 2) some degree of preferential evaporation of D and ^{18}O during infiltration, 3) hydrothermal water-rock interactions in high-temperature regions of the groundwater system, or 4) a combination of these effects. Five of the eight precipitation collectors deployed by Fackrell et al. (2020) were replicated to within 1.5 km, three of which were identical placements. Fackrell et al. (2020) concluded that rainfall sourced at higher elevations, possibly from the slopes of Mauna Kea or Mauna Loa, are recharging into the Hualālai aquifers. In order to test this conclusion, we strategically placed precipitation collectors at higher elevations.

We computed combined VWA for the five replicated sites, which resulted in better characterization of the groundwater data presented in previous literature (Tillman et al., 2014; Kelly and Glenn, 2015; Fackrell et al., 2020). The 2012–2014 sampling period of Fackrell et al. (2020) remained relatively neutral, however the 2017–2019 study period experienced both a La Niña from October 2017 to March 2018 and an El Niño from October 2018 to June 2019 (NOAA National, 2021). Previous work in Hawai'i observed lower than normal rainfall during El Niño, which can be further exacerbated by the influence of the Pacific Decadal Oscillation (PDO) (Chu and Chen, 2005; Giambelluca et al., 2013; Frazier and Giambelluca, 2017; Elison Timm et al., 2020). Changes in the atmospheric circulation, resulting in strong surface westerly anomalies, have been observed to reduce trade wind rainfall in Hawai'i (e.g., Chu and Chen, 2005). We hypothesize that the two LMWL represent ends of a spectrum, due to such variability in atmospheric and climate processes in this region. However, specific investigations into the cause of such variability is beyond the scope of this project.

Long-term variations, such as those shown above, have not been previously observed, and highlight the need for long-term sampling in order to accurately characterize rainfall for groundwater recharge studies. To our knowledge, the longest collection of isotope data in Hawai'i was conducted by the International Atomic Energy Agency, through the Global Network of Isotopes in Precipitation (GNIP). Through this project, data for only a few years (1962–1969) and from a single station was collected. We hope, however, that the results presented here will serve as motivation for the creation of long-term monitoring of water isotopes in Hawai'i.

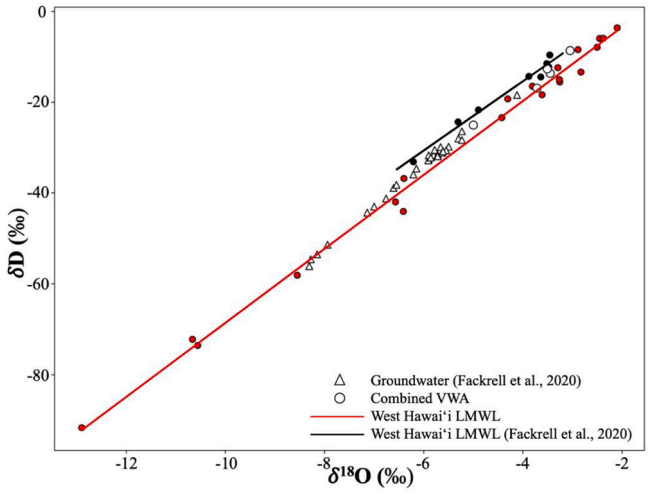

Fig. 6. Comparison of the local meteoric water line (LMWL) defined by Fackrell et al. (2020) in black, the LMWL defined by this study in red, a combined VWA of overlapping sites in white circles, and groundwater collected and analyzed by Fackrell et al. (2020) as white triangles.

3.3. Variability of ions in precipitation

The investigation into bulk deposition for the West Hawai'i study area, specifically chloride and sulfate concentrations, is to explore whether our results are similar to those of previous studies that observed increased aerosols downwind of a volcano contributing to the development of acid rain (Eriksson, 1957; Miller and Yoshinaga, 1981; Harding and Miller, 1982; Nachbar-Hapai et al., 1989; Siegel et al., 1990; Scholl and Ingebritsen, 1995), however direct comparison is difficult due to the large spatial difference between the focus of the previous studies on East Hawai'i and ours in West Hawai'i. Major ion concentrations as bulk (wet + dry) deposition for each sampling trip are reported in Tachera (2020).

Quarterly cumulative rainfall in low- and mid-elevations was relatively low (less than 250 mm) for each sampling period prior to, and during, the 2018 Kīlauea LERZ eruption (Fig. 7). After the eruption ended in September 2018, precipitation amounts increased to 500 mm or higher. The low rainfall observations during the Kīlauea eruption, particularly below the inversion layer, corroborate those of Zuo et al. (2020), who present rainfall and gas emission data in parallel with a numerical model suggesting reduced rainfall during periods of increased aerosols.

Spikes in chloride and sulfate concentrations (μM) were observed during two periods: 1) June 2018 to August 2018 and 2) November 2018 to March 2019. The first spike coincided with the 2018 Kīlauea eruption, which caused heavy vog in West Hawai'i. Low rainfall (less than 250 mm precipitation) was also observed at all sites during this time, despite coinciding with the typical wet season for West Hawai'i. The second spike was observed in only a few sites and was more pronounced for chloride than sulfate. Again, quarterly cumulative rainfall measurements did not exceed ~250 mm for all sites, however November to March is the expected dry season for West Hawai'i. Previous studies have also observed higher major ion concentrations during periods of lower rainfall (e.g., Lee et al., 2000).

3.4. Event-based impacts on precipitation

Two events during our study period affected the chemistry of precipitation: 1) the lower East Rift Zone (LERZ) eruption of Kīlauea Volcano from May to September 2018, and 2) Hurricane Lane, which dissipated into a tropical storm upon approach to the Hawaiian Islands in August 2018. To better understand the impacts of these events on the ion concentrations in rainfall, we compared chloride and sulfate concentrations to sodium concentrations (Fig. 8a and 8b). Stable isotopic compositions were also investigated (Fig. 8c).

The observed chloride concentrations approximated those of seawater, with the largest deficiencies occurring at lower

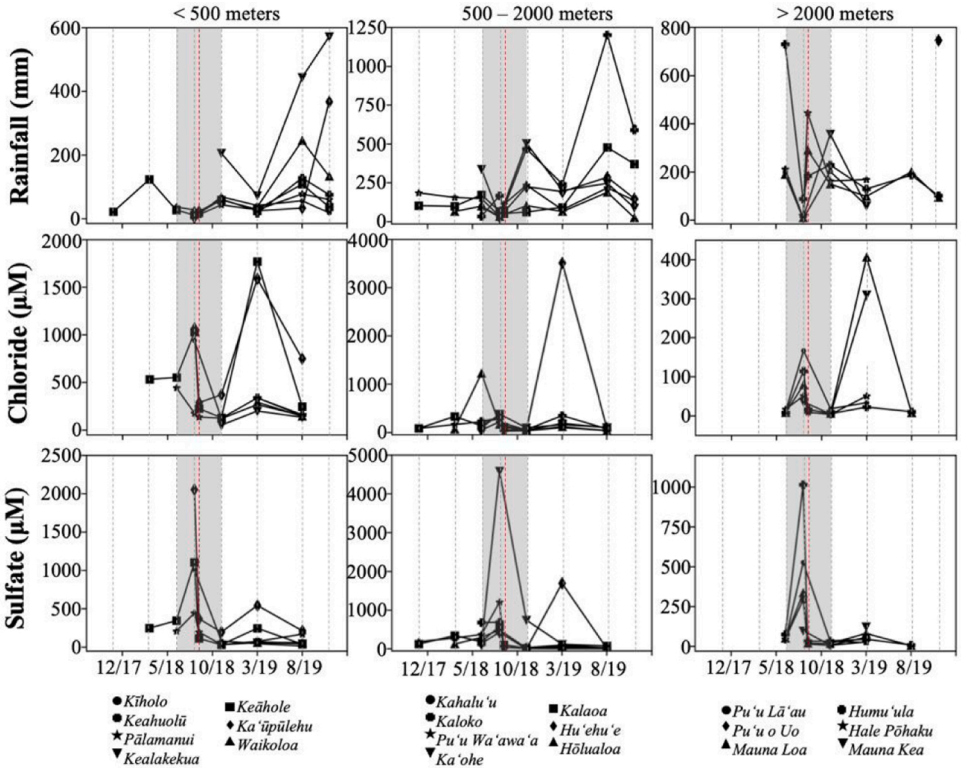

Fig. 7. Precipitation (mm), chloride (μM), and sulfate (μM) concentrations for precipitation sites sampled between August 2017 and August 2019. Shaded region represents the 2018 Kīlauea East Rift Zone eruption period. Dashed vertical lines represent each sample collection, and the red vertical dashed line represents the Hurricane Lane event and sample collection.

concentrations, particularly the samples collected during Hurricane Lane (Fig. 8a). This may be attributed to the low chloride and sodium concentrations approaching the detection limits, as similar observations were made in previous studies (e.g., Scholl and Ingebritsen, 1995). Crustal dust could also cause the sodium concentrations to increase relative to chloride (Keene et al., 1986; Scholl and Ingebritsen, 1995), however indicators like Al and Fe were not collected during this study therefore we are unable to determine if the higher abundance of sodium is due to this deposition. Chloride concentrations do not appear to be affected by the 2018 Kīlauea eruption, as the spread of pre-, during-, and post-eruption samples were similar. A Welch's *t*-test performed on pre-during ($p = 0.535$),

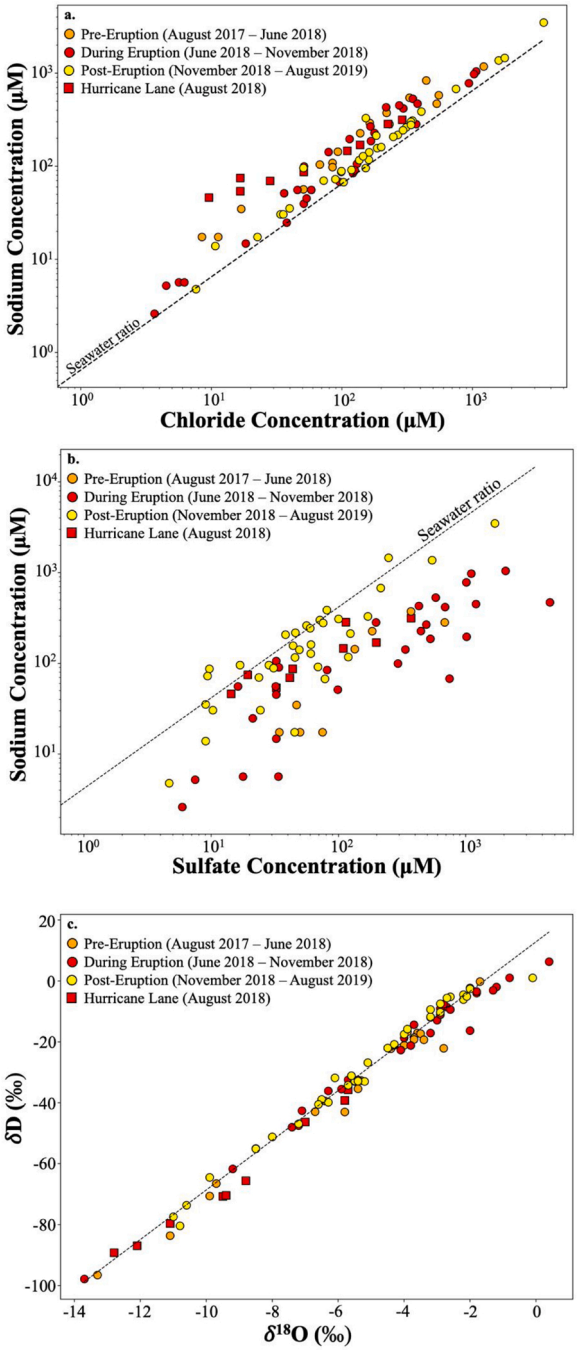

Fig. 8. (a) chloride compared to sodium concentrations (µM), with the seawater ratio; (b) sulfate compared to sodium concentrations (µM), with the seawater ratio; (c) isotopic composition (‰) with the local meteoric water line. Points are colored as: before the 2018 Kīlauea eruption (orange), during the eruption (red), and after the eruption ended (yellow). Hurricane Lane samples are plotted as red squares (red, as sampled during the eruption). Data are shown on a log-log scale.

during-post ($p = 0.151$) and pre-post ($p = 0.349$) groups concluded there is no statistical difference between the samples.

Sulfate concentrations exceeded the seawater ratio even at the start of our sampling due to the long-term Puʻu ʻŌʻō eruption of Kīlauea Volcano, which began in 1983 and terminated just prior to the start of the 2018 Kīlauea LERZ eruption (Fig. 8b). Between March 2014 and December 2017, daily summit and East Rift Zone sulfur dioxide emission rates were between 1,227 and 9,970 metric tonnes per day (t/d), averaging 4,783 t/d (Elias et al., 2018). This emission rate dramatically increased during the 2018 Kīlauea lower East Rift Zone eruption. Preliminary analyses from the U.S. Geological Survey indicate that sulfur dioxide gas emissions averaged more than 50,000 tons per day and during some periods exceeded 100,000 tons per day (Williams et al., 2020). During the 2018 Kīlauea eruption, Hurricane Lane impacted the State of Hawaiʻi in August 2018, during which sulfate concentrations also exceeded the seawater ratio. The Lane samples also display the lowest sulfate concentrations observed during the eruption. After the cessation of the 2018 Kīlauea eruption, sulfate concentrations decreased approximately 70 % to yield chloride ratios approaching those in seawater. A Welch's *t*-test performed on the sulfate concentrations concluded that there is a statistical difference between during-post groups ($p = 0.032$, $\alpha = 0.05$), however there is no statistical difference between pre-during ($p = 0.118$) and pre-post ($p = 0.159$) groups.

Downwind of the volcano, ammonium sulfate is typically observed due to the reaction of terrigenous and volcanic ammonia and the sulfate compounds in the atmosphere (Cornell et al., 2001). Tachera (2020) reports the ammonium concentrations observed during this study, demonstrating that the highest concentrations of ammonium ion during our study period were recorded during the 2018 Kīlauea eruption.

Stable isotopic compositions before, during, and after the eruption are spread throughout the range of samples (Fig. 8c). Rainfall during the hurricane was less than 200 mm at low- to mid-elevations, and was between 200–400 mm at high-elevations. Although the rainfall amounts were not notable at low elevations, samples collected during Hurricane Lane observed the most depleted isotopic compositions observed during our study period for this elevation interval. A Welch's *t*-test performed on the isotopic compositions shows that there is no statistical difference between the pre-during ($p = 0.686$), during-post ($p = 0.781$), and pre-post ($p = 0.511$) groups.

4. Conclusions

Samples of precipitation were collected at 20 sites from Central to West Hawaiʻi between August 2017 and November 2019. The isotopic composition and bulk ion deposition of such samples were measured and compared to previous studies conducted on Hawaiʻi Island and Maui to better characterize the source of groundwater in Central to West Hawaiʻi Island. Significant findings support our assertion that long-term precipitation data are crucial when developing a LMWL for Hawaiʻi. These findings include:

- The local meteoric water line established during this study is similar to those for East Hawaiʻi and East Maui, as well as the global meteoric water line. It differs from the local meteoric water line established in the previous West Hawaiʻi study by Fackrell et al. (2020). Combined VWA for replicated sites produce averages that better characterize the groundwater isotopic compositions observed in previous studies. Long-term studies are needed to better understand the variations observed in the meteoric water lines spanning a near-decade long sampling of these sites.
- The $\delta^{18}O$ isotope-elevation relationship established for West Hawaiʻi is similar to the trade wind (for low- and mid- elevations) and high-elevation relationships observed in East Hawaiʻi. Depletion in VWA $\delta^{18}O$ is observed in sites within low annual rainfall areas (less than 750 mm) relative to the isotope-elevation regression. These sites possibly experience rainfall mainly during extratropical and subtropical storms, which already have depleted $\delta^{18}O$ compositions. Enrichment in VWA $\delta^{18}O$ is observed for sites in the rain band, which wraps around the southern tip of Hawaiʻi Island and flows up the leeward slopes of Mauna Loa and Hualālai.

Additional results provide insight into extreme events, which can impact the chemical composition of precipitation. These findings include:

- During periods of low rainfall (less than 250 mm), as well as the 2018 Kīlauea eruption, all sites observed increased concentrations of sulfate and chloride. Precipitation at low- and mid- elevation sites remained low during the 2018 Kīlauea eruption, supporting previous research that an increase in aerosols decreases rainfall downwind of the volcano.
- Sulfate concentrations increased during the Kīlauea eruption, however chloride concentrations did not. Welch's t-tests demonstrated a statistical difference only between sulfate concentrations observed during and after the eruption ended ($p = 0.032$), and no statistical difference between the rest of the samples.

This paper provides a foundation to follow-on work including: 1) incorporation of the data presented herein with new groundwater chemistry data in order to investigate the recharge zones, interconnectivity, and storage of West Hawaiʻi aquifers; and 2) analyses of the effects of seasalt aerosol deposition on ecological processes and water quality. Continued collection of bulk deposition, particularly in the current quiet period of Kīlauea Volcano, would aid in understanding the importance and impacts of volcanic emissions on rainfall rates and compositions. Multi-decadal sampling, although challenging, will be crucial to determining the variability of stable isotopes in precipitation.

Funding

The views expressed are those of the author(s) and do not necessarily reflect the views of any of the agencies listed. This project has

been funded by the NSF Hawai'i EPSCoR Program through the National Science Foundation's Research Infrastructure Improvement award (RII) Track-1: 'Ike Wai: Securing Hawai'i's Water Future Award # OIA-1557349. G.T. is supported by NSF Grant AGS-1945972.

CRediT authorship contribution statement

Diamond K. Tachera: Conceptualization, Methodology, Software, Formal analysis, Investigation, Data curation, Writing - original draft, Visualization, Project administration. **Nicole C. Lautze:** Resources, Writing - review & editing, Supervision, Project administration, Funding acquisition. **Giuseppe Torri:** Validation, Formal analysis, Resources, Writing - review & editing. **Donald M. Thomas:** Conceptualization, Methodology, Validation, Formal analysis, Resources, Writing - review & editing.

Declaration of Competing Interest

The authors declare that they have no known competing financial interests or personal relationships that could have appeared to influence the work reported in this paper.

Acknowledgements

The authors would like to thank the West Hawai'i community, Hui Aloha Kīholo, The Nature Conservancy, Rebecca Most, Barbara Seidel, Keith Olson, Pamela Madden, the Natural Energy Laboratory of Hawai'i Authority, Mana Purdy, the Queen Lili'uokalani Trust, David Chai, Hualālai Resort, University of Hawai'i Pālamanui Campus, Tommy and Nina Segovia, Nāmaka Whitehead, Billy Lee, Keala Kanaka'ole, Colin Onaka, Kamehameha Schools, Hui Kuahiwi, Gregory Chun, Ardele Kershaw, Hu'ehu'e Ranch, Paul Ponthieux, Henk Rogers, Pu'u Wa'awa'a Ranch, Britt Craven, Palani Ranch, Department of Land and Natural Resources Division of Forestry and Wildlife, Brian Shiro, Michaela Musilova, University of Hawai'i HI-SEAS, Fritz Klasner, Mike Yabe, Office of Maunakea Management, Aidan Colton, and the Mauna Loa Observatory for providing access and support for sampling locations. The authors also thank Honour Booth, Daniel Dores, Henrietta Dulai, Kiana Frank, Keku'iapōiula Keliipuleole, Trista McKenzie, Brytne Okuhata, Kexin Catherine Rong, Chris Shuler, Natalie Wallsgrove, Sheree Watson, and Taylor Viti for their assistance with sampling and data analysis. This paper was improved by constructive suggestions from two anonymous reviewers. This paper is SOEST Contribution #11243.

Appendix A. Supplementary data

Supplementary material related to this article can be found, in the online version, at doi:https://doi.org/10.1016/j.ejrh.2021.100786.

References

Aiuppa, A., Bellomo, S., Brusca, L., D'Alessandro, W., Di Paola, R., Longo, M., 2006. Major-ion bulk deposition around an active volcano (Mt. Etna, Italy). Bull. Volcanol. 68, 255–265. https://doi.org/10.1007/s00445-005-0005-x.

Attias, E., Thomas, D., Sherman, D., Ismail, K., Constable, S., 2020. Marine electrical imaging reveals novel freshwater transport mechanisms in Hawai'i. Sci. Adv. 6, 1–8.

Cerón, R.M., Cerón, J.G., Córdova, A.V., Zavala, J., Muriel, M., 2005. Chemical composition of precipitation at coastal and marine sampling sites in Mexico. Global NEST Journal 7 (2), 212–221.

Chu, P.S., Chen, H., 2005. Interannual and interdecadal rainfall variations in the Hawaiian Islands. J. Clim. 18, 4796–4813.

Cornell, S., Mace, K., Coeppicus, S., Duce, R., Huebert, B., Jickells, T., Zhuang, L.Z., 2001. Organic nitrogen in Hawaiian rain and aerosol. J. Geophys. Res. Atmos. 106 (D8), 7973–7983. https://doi.org/10.1029/2000JD900655.

Craig, H., 1961. Isotopic variations in meteoric waters. Science 133 (3465), 1702–1703. https://doi.org/10.1126/science.133.3465.1702.

Dansgaard, W., 1964. Stable isotopes in precipitation. Tellus 16 (4), 436–4468. https://doi.org/10.3402/tellusa.v16i4.8993.

Dores, D., Glenn, C.R., Torri, G., Whittier, R.B., Popp, B.N., 2020. Implications for groundwater recharge from stable isotopic composition of precipitation in Hawai'i during the 2017-2018 La Nina. Hydrol. Process. https://doi.org/10.1002/hyp.13907.

Dütch, M., Pfahl, S., Wernli, H., 2016. Drivers of δ2H variations in an idealized extratropical cyclone. Geophys. Res. Lett. 43, 5401–5408. https://doi.org/10.1002/2016GL068600.

Elias, T., Kern, C., Horton, K., Gabriel, H., Sutton, A.J., 2018. SO2 emission rates from Kilauea Volcano, Hawaii (2014-2017). U.S. Geological Survey data release. https://doi.org/10.5066/F7794402.

Elison Timm, O., Li, S., Liu, J., Beilman, D.W., 2020. On the changing relationship between North Pacific climate variability and synoptic activity over the Hawaiian Islands. Int. J. Climatol. 1–17. https://doi.org/10.1002/joc.6789.

Eriksson, E., 1957. The chemical composition of hawaiian rainfall. Tellus 9 (4), 509–520. https://doi.org/10.3402/tellusa.v9i4.9125.

Fackrell, J.K., Glenn, C.R., Thomas, D., Whittier, R., Popp, B.N., 2020. Stable isotopes of precipitation and groundwater provide new insight into groundwater recharge and flow in a structurally complex hydrogeologic system: west Hawai'i. USA. Hydrogeology Journal 28 (4), 1191–1207. https://doi.org/10.1007/s10040-020-02143-9.

Frazier, A.G., Giambelluca, T.W., 2017. Spatial trend analysis of Hawaiian rainfall from 1920 to 2012. Int. J. Climatol. 37 (5), 2522–2531. https://doi.org/10.1002/joc.4862.

Friedman, I., Woodcock, A.H., 1957. Determination of deuterium-hydrogen ratios in Hawaiian waters. Tellus 9 (4), 553–556. https://doi.org/10.3402/tellusa.v9i4.9119.

Gedzelman, S.D., Lawrence, J.R., 1990. The isotopic composition of precipitation from two extratropical cyclones. American Meteorological Society Monthly Weather Review 118, 495–509 doi: 10.1175/1520-0493(1990)118<0495:TICOPF>2.0.CO;2.

Giambelluca, T.W., Chen, Q., Frazier, A.G., Price, J.P., Chen, Y., Chu, P., Eischeid, J.K., Delparte, D.M., 2013. Online rainfall atlas of Hawaii. Bull. Am. Meteorol. Soc. 94 (3), 313–316. https://doi.org/10.1175/BAMS-D-11-00228.1.

Giambelluca, T.W., Shuai, X., Barnes, M.L., Alliss, R.J., Longman, R.J., Miura, T., Chen, Q., Frazier, A.G., Mudd, R.G., Cuo, L., Businger, A.D., 2014. Evapotranspiration of Hawai'i. Final report submitted to the U.S. Army Corps of Engineers - Honolulu District, and the Commission of Water Resource Management. Hawaii Revis. Statut. Hawaii.

Godoy, J.M., Godoy, M.L.D.P., Neto, A., 2012. Direct determination of δ(D) and δ(18O) in water samples using cavity ring down spectrometry: Application to bottled mineral water. J. Geochem. Explor. 119-120, 1–5. https://doi.org/10.1016/j.gexplo.2012.05.007.

Good, S.P., Mallia, D.V., Lin, J.C., Bowen, G.J., 2014. Stable isotope analysis of precipitation samples obtained via crowdsourcing reveals the spatiotemporal evolution of superstorm sandy. PLoS One 9 (3), 1–7. https://doi.org/10.1371/journal.pone.0091117.

Harding, D., Miller, J.M., 1982. The influence on rain chemistry of the Hawaiian Volcano Kilauea. J. Geophys. Res. Oceans 87 (C2), 1225–1230. https://doi.org/10.1029/JC087iC02p01225.

Hautman, D.P., Munch, D.J., 1997. Method 300.0, Revision 1.0: Determination of Inorganic Anions in Drinking Water by Ion Chromatography. National Exposure Research Laboratory Office of Research and Development. U.S. Environmental Protection Agency, Cincinnati, 40 p.

Keene, W.C., Pszenny, A.A.P., Galloway, J.N., Hawley, M.E., 1986. Sea-salt corrections and interpretation of constituent ratios in marine precipitation. J. Geophys. Res. 91 (D6), 6647–6658.

Kelly, J.L., Glenn, C.R., 2015. Chlorofluorocarbon apparent ages of groundwaters from west Hawaii, USA. J. Hydrol. 527, 355–366. https://doi.org/10.1016/j.jhydrol.2015.04.069.

Kong, Y., Pang, Z., 2016. A positive altitude gradient of isotopes in the precipitation over the Tianshan Mountains: effects of moisture recycling and sub-cloud evaporation. J. Hydrol. (Amst) 542, 222–230. https://doi.org/10.1016/j.jhydrol.2016.09.007.

Lee, B.K., Hong, S.H., Lee, D.S., 2000. Chemical composition of precipitation and wet deposition of major ions on the Korean peninsula. Atmos. Environ. 34, 563–575. https://doi.org/10.1016/S1352-2310(99)00225-3.

Leopold, L.B., 1949. The interaction of trade wind and sea breeze. Hawaii. Journal of Meteorology 6, 312–320.

Miller, J.M., Yoshinaga, A.M., 1981. The pH of Hawaiian precipitation, a preliminary report. Geophys. Res. Lett. 8, 779–782. https://doi.org/10.1029/GL008i007p00779.

Moore, J.G., Clague, D.A., 1992. Volcano growth and evolution of the island of Hawaii. Geol. Soc. Am. Bull. 104, 1471–1484.

Nachbar-Hapai, M., Siegel, B.Z., Russell, C., Siegel, S.M., Siy, M.L., Priestley, D., 1989. Acid rain in the Kilauea Volcano area (Hawaii). Arch. Environ. Contam. Toxicol. 18, 65–73. https://doi.org/10.1007/BF01056191.

Neal, C.A., Anderson, K.R., 2020. Preliminary Analyses of Volcanic Hazards at Kīlauea Volcano, Hawai'i, 2017-2018. U.S. Geological Survey Open File Report 2020-1002.

NOAA National, 2021. Weather Service Climate Prediction Center. Cold & Warm Episodes by Season. https://origin.cpc.ncep.noaa.gov/products/analysis_monitoring/ensostuff/ONI_v5.php.

Oki, D.S., 1999. Geohydrology and Numerical Simulation of the Ground-Water Flow System of Kona, Island of Hawaii. U.S. Geological Survey Water-Resources Investigations Report, pp. 99–4073.

Paternoster, M., Liotta, M., Favara, R., 2008. Stable isotope ratios in meteoric recharge and groundwater at Mt. Vulture volcano, southern Italy. Journal of Hydrology 348, 87–97. https://doi.org/10.1016/j.jhydrol.2007.09.038.

Poage, M.A., Chamberlain, C.P., 2001. Empirical relationships between elevation and the stable isotope composition of precipitation and surface waters: considerations for studies of paleoelevation change. Am. J. Sci. 301, 1–15. https://doi.org/10.2475/ajs.301.1.1.

Scholl, M.A., Ingebritsen, S.E., 1995. Total Non-seasalt Sulfate and Chloride Measured in Bulk Precipitation Samples From the Kilauea Volcano Area, Hawaii. U.S. Geological Survey Water-resources Investigations Report, pp. 95–4001.

Scholl, M.A., Ingebritsen, S.E., Janik, C.J., Kauahikaua, J.P., 1996. Use of precipitation and groundwater isotopes to interpret regional hydrology on a tropical volcanic island: kilauea volcano area. Hawaii. Water Resources Research 32 (12), 3525–3537. https://doi.org/10.1029/95WR02837.

Scholl, M.A., Gingerich, S.B., Tribble, G.W., 2002. The influence of microclimates and fog on stable isotope signatures used in interpretation of regional hydrology: east Maui, Hawaii. Journal of Hydrology 264, 170–184. https://doi.org/10.1016/S0022-1694(02)00073-2.

Scholl, M.A., Giambelluca, T.W., Gingerich, S.B., Nullet, M.A., Loope, L.L., 2007. Cloud water in windward and leeward mountain forests: the stable isotope signature of orographic cloud water. Water Resour. Res. 43, 1–13. https://doi.org/10.1029/2007WR006011.

Siegel, B.Z., Nachbar-Hapai, M., Siegel, S.M., 1990. The contribution of sulfate to rainfall pH around Kilauea Volcano. Hawaii. Water, Air, and Soil Pollution 52, 227–235. https://doi.org/10.1007/BF00229435.

Sutton, A.J., Elias, T., 2014. One hundred volatile years of volcanic gas studies at the hawaiian volcano observatory. Characteristics of Hawaiian Volcanoes. U.S. Geological Survey Professional Paper 1801-7, pp. 295–302. https://doi.org/10.3133/pp18017.

Tachera, D., 2020. Kona precipitation chemistry data for all sampling trips. HydroShare. https://doi.org/10.4211/hs.032c377f981c4ce9b6e8ba75778507dd.

Taylor, B., 2019. Shoreline slope breaks revise understanding of hawaiian shield volcanoes evolution. Geochem. Geophys. Geosystems 20, 4025–4045. https://doi.org/10.1029/2019GC008436.

Tillman, F.D., Oki, D.S., Johnson, A.G., Barber, L.B., Beisner, K.R., 2014. Investigation of geochemical indicators to evaluate the connection between inland and coastal groundwater systems near Kaloko-Honokōhau National Historical Park, Hawai'i. Appl. Geochem. 51, 278–292. https://doi.org/10.1016/j.apgeochem.2014.10.003.

Torri, G., Ma, D., Kuang, Z., 2017. Stable water isotopes and large-scale vertical motions in the tropics. J. Geophys. Res. Atmos. 122, 1–15. https://doi.org/10.1002/2016JD026154.

Williams, D.M., Avery, V.F., Coombs, M.L., Cox, D.A., Horwitz, L.R., McBride, S.K., McClymont, R.J., Moran, S.C., 2020. U.S. Geological Survey 2018 Kīlauea Volcano Eruption Response in Hawai'i - After-action Review. U.S. Geological Survey, Open-file Report 2020-1041, 56 p.

Zuo, T., Nugent, A.D., Thompson, G., 2020. Volcanic aerosol emission impacts on orographic precipitation in Hawaii. 13-17 July 2020. 19th Conference on Mountain Meteorology Virtual Meeting.